Catalytic Mechanism of Penicillin-Binding Protein 5 of *Escherichia coli*†

Weilie Zhang, Qicun Shi, Samy O. Meroueh, Sergei B. Vakulenko, and Shahriar Mobashery*

Department of Chemistry and Biochemistry, University of Notre Dame, Notre Dame, Indiana 46556

Received April 25, 2007; Revised Manuscript Received June 5, 2007

ABSTRACT: Penicillin-binding proteins (PBPs) and β-lactamases are members of large families of bacterial enzymes. These enzymes undergo acylation at a serine residue with their respective substrates as the first step in their catalytic events. Penicillin-binding protein 5 (PBP 5) of *Escherichia coli* is known to perform a DD-carboxypeptidase reaction on the bacterial peptidoglycan, the major constituent of the cell wall. The roles of the active site residues Lys47 and Lys213 in the catalytic machinery of PBP 5 have been explored. By a sequence of site-directed mutagenesis and chemical modification, we individually introduced γ-thialysine at each of these positions. The pH dependence of k_{cat}/K_m and of k_{cat} for the wild-type PBP 5 and for the two γ-thialysine mutant variants at positions 47 and 213 were evaluated. The pH optimum for the enzyme was at 9.5−10.5. The ascending limb to the pH optimum is due to Lys47; hence, this residue exists in the free-base form for catalysis. The descending limb from the pH optimum is contributed to by both Lys213 and a water molecule coordinated to Lys47. These results have been interpreted as Lys47 playing a key role in proton-transfer events in the course of catalysis during both the acylation and deacylation events. However, the findings for Lys213 argue for a protonated state at the pH optimum. Lys213 serves as an electrostatic anchor for the substrate.

β-Lactamases and penicillin-binding proteins (PBPs[1]) constitute a group of related proteins. With the exception of the class B β-lactamases and a single known PBP, which are zinc dependent, all these proteins undergo acylation at a serine residue with their respective substrates. The minimal motif for this acylation apparatus is the sequence Ser-X-X-Lys, with Ser being the site of acylation. The amino acid sequence identity among these proteins is low, yet the catalytic domains have retained the same folding pattern (*1*−*3*). Working with this conserved structural template, that is, the shared protein folding, nature has diversified function in a most impressive manner. Three distinct hydrolytic deacylation mechanisms with β-lactam antibiotics have evolved for the serine-dependent β-lactamases (*4*). Furthermore, PBPs have evolved transpeptidation and DD-carboxypeptidation reactions, which perform the final steps in the maturation of the peptidoglycan components of the bacterial cell wall. The unique protein fold has proven itself versatile.

Because of the distinct reactions that have evolved around the catalytic Ser-X-X-Lys sequence motif, the incremental contributions to the catalytic steps of each of these enzymic reactions by the conserved active site residues are different. It would be informative to dissect the catalytic steps in each case to shed light on how these reactions have emerged from the same structural fold shared by all these enzymes. We describe herein our efforts in investigations of the mechanism of action of penicillin-binding protein 5 (PBP 5) of *Escherichia coli*. This enzyme is known to perform a DD-carboxypeptidase reaction on the bacterial peptidoglycan, the major constituent of the cell wall. The peptidoglycan is made up of a repeating backbone of *N*-acetylglucosamine (NAG) and *N*-acetylmuramic acid (NAM) with an appended peptide stem. The three-dimensional structure of the peptidoglycan was solved recently, indicating a right-handed helix for the sugar backbone and a largely unstructured peptide portion (*5*). The peptide stem is typically a pentapeptide, with a number of unusual features such as a D-Glu residue with a peptide bond via its side chain carboxylate. Diaminopimelate is the third amino acid, and two D-Ala residues are at the C-terminal site. The structure of the repeating unit is given in Figure 1 (structure **1**). PBP 5 hydrolyzes the peptide bond between the two D-Ala residues, in a two-step process. In the first step, the active-site serine is acylated (structure **2**) and in the next step, the acyl-enzyme species is hydrolyzed, resulting in a peptidoglycan whose peptide is lacking the terminal D-Ala (structure **3**). Because the presence of the terminal D-Ala in peptidoglycan is required for the critical cell wall cross-linking reaction of transpeptidases, one physiological role for PBP 5 in *E. coli* is moderation of the degree of cross-linking. This enzyme is also implicated in the maintenance of the cell shape (*6*).

We have investigated the roles of Lys47 and Lys213 in the catalytic machinery of PBP 5 in this article. The former is the lysine in the Ser-X-X-Lys motif, which is conserved in all PBPs and serine-dependent β-lactamases. The second

† This research was supported by a grant from the National Institutes of Health. Simulations were performed on the University of Notre Dame Biocomplexity Cluster supported in part by NSF MRI Grant No. DBI-0420980.

* Corresponding author. Tel: (574) 631-2933. Fax: (574) 631-6652. E-mail: mobashery@nd.edu.

[1] Abbreviations: PBP, penicillin-binding protein; twtPBP 5, truncated wild-type PBP 5; tPBP 5, truncated Cys115Ser mutant PBP 5; γtPBP 5, γ-thialysine variants of tPBP 5, IPTG, isopropyl-β-D-thiogalactoside; DTNB, 5,5′-dithiobis-2-nitrobenzoic acid; HRP, horseradish peroxidase; FAD, Flavin adenine dinucleotide; DAO, D-amino acid oxidase; AMPSO, *N*-(1,1-dimethyl-2-hydroxyethyl)-3-amino-2-hydroxypropanesulfonic acid.

10.1021/bi700777x CCC: $37.00
Published on Web 08/09/2007

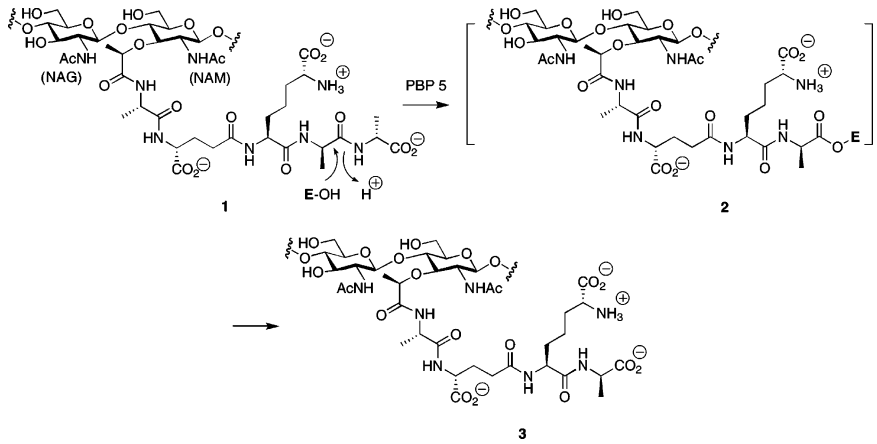

FIGURE 1: Turnover of the bacterial peptidoglycan catalyzed by penicillin-binding protein 5 of *E. coli*. The enzyme experiences acylation and deacylation in the course of the hydrolytic reaction.

is another active site residue. The roles of the corresponding residues in class A β-lactamases have been scrutinized because a debate has ensued on the nature of its protonation state (*7*; and the citations given therein). Evidence presented herein indicates that Lys47 of PBP 5 is involved in proton transfer in the course of the catalytic turnover events, and Lys213 serves as the electrostatic anchor for the terminal carboxylate of the substrate.

EXPERIMENTAL PROCEDURES

Materials. All restriction enzymes and other DNA-modifying enzymes were from New England Biolabs or Stratagene. CH Sepharose 4B resin, D-Ala, horseradish peroxidase (HRP, Type X), ampicillin, kanamycin, flavin adenine dinucleotide (FAD), D-amino acid oxidase (DAO), Triton X-100, Mes, Cap, 5,5′-dithiobis-2-nitrobenzoic acid (DTNB), and the PBP 5/carboxypeptidase substrate diacetyl-L-Lys-D-Ala-D-Ala were purchased from Sigma. The QuantaBlu substrate solution was from Pierce Chemical Co. Isopropyl-β-D-thiogalactoside (IPTG) and the LB Broth were purchased from Fisher Scientific.

Generation of Truncated PBP 5 and Mutant PBP 5 Variants. *Dac*A gene for mature PBP 5 was amplified by PCR from the chromosome of *E. coli* K12 using two custom-synthesized primers, EcPBP5Nde, 5′-ATCATATGGATGACCTGAATATCAAAACTATG-3′ and PBP5EcR, 5′-TATAAGCTTAGTTACCTTCCGGGATTTCTTGCAAC-3′, to remove its 18-amino-acid carboxy terminal anchor and the 29-residue-long amino terminal signal peptide. The resulting product was cloned into the *Nde*I and *Hind*III sites in the polylinker of the pET24a(+) vector under the T7 promoter. To clone PBP 5 lacking domain 2, the *dac*A gene of *E. coli* was PCR-amplified from the pET24a(+) vector using two custom-made primers: EcPBP5Nde, 5′-ATCATATGGATGACCTGAATATCAAAACTATG-3′ and Ec5-Dom1, 5′-ATAAAGCTTAAAAGAAACGGAAGCCCCAGGTTAGC-3′ (*Nde*I and *Hind*III sites underlined). The PCR product was digested by the *Nde*I and *Hind*III, ligated into the polylinker of the pET24a(+) vector and transformed into *E. coli* JM83. The selection of transformants was performed on LB agar supplemented with ampicillin (100 μg/mL). The nucleotide sequences of *dac*A gene from several transformants were verified by sequencing both DNA strands. Then, the construct was transformed into *E. coli* BL21(DE3) cells. The resulting PBP 5 gene encodes a soluble form of PBP 5 that lacks domain 2 (residues 263−356) of its carboxyl terminus.

Generation of the Cys115Ser mutant and the two double mutant variants. Lys47Cys/Cys115Ser and Lys213Cys/Cys115Ser, was accomplished by using a QuikChange site-directed mutagenesis kit (Stratagene), in accordance with the manufacturer's recommendations. First, Cys115 was mutated to serine utilizing the following primers: Cys115D (5′-GGTAACGATGCTTCTGTCGCCATGGCC-3′; mutated codon underlined) and Cys115R (5′-GGCCATGGCGACAGAAGCATCGTTACC-3′). Then, Lys47 or Lys213 was mutated to cysteine using primers Lys47D (5′- CCTGCCAGCCTGACCTGCATGATGACCAGTTAC-3′) and Lys47R (5′-GTAACTGGTCATCATGCAGGTCAGGCTGGCAGG-3′) or primers Lys213D (5′-GAATGTCGACGGCATCTGCACCGGACACACTGAC-3′) and Lys213R (5′-GTCAGTGTGTCCGGTGCAGATGCCGTCGATATTC-3′; mutated codons underlined), respectively. Nucleotide sequences of mutants were confirmed by sequencing both DNA strands. After recloning mutant genes into the *Nde*I-*Hind*III sites of expression vector pET24a(+), constructs were transformed into the *E. coli* BL21 (DE3) cells for protein expression.

Purification of Soluble PBP 5 Variants. Purification of the truncated wild-type PBP 5 (twtPBP 5) and truncated Cys115Ser mutant PBP 5 (tPBP 5) was according to a modification of a literature procedure (*8*). Cells were incubated overnight in 5 mL of LB medium supplemented with 30 μg/mL of kanamycin. Cells were diluted into 500 mL of fresh kanamycin-supplemented (30 μg/mL) LB medium and growth was continued with mixing (135 rpm) at 37 °C until the culture reached an OD600 of 0.8. IPTG was added at this stage to a concentration of 0.4 mM, and the culture was incubated at 20 °C for an additional 12 h. All subsequent steps were performed at 4 °C. Cells were harvested by centrifugation at 3000*g* for 10 min, resuspended in 20 mM Tris and 0.1% Triton X-100 at pH 8.0, and disrupted by 30 cycles of sonication (30 s of burst and 20 s of rest for each cycle) using a Branson sonifier. Bacterial cell debris was removed using a Beckman-Coulter TJ-25 centrifuge at 21,000*g* for 40 min.

The supernatant from the twtPBP 5 or tPBP 5 were mixed with the chromatographic resin CH Sepharose 4B, which was

previously coupled with ampicillin (Ampicillin/CH-Sepharose 4B was prepared by mixing 600 mg of ampicillin with 10 mL of an aqueous suspension containing 3.5 g of activated CH-Sepharose 4B for 3.5 h at 30 °C). The protein-binding step was performed on a shaker at room temperature for 30 min. The resin was transferred onto a sintered glass filter and was washed with 1 L of Tris buffer (20 mM Tris, 1 M NaCl, and 0.1% Triton X-100 at pH 7.5) at 4 °C for 30 min. The desired protein was eluted using 0.5 M Tris and 1 M NH_2OH at pH 7.0. The elution buffer was added directly to the resin on the sintered glass filter. The resin was gently stirred for 20 min at room temperature and then separated from the liquid by filtration. The filtrate containing PBP 5 or its Cys115Ser mutant was dialyzed against 25 mM $NaHCO_3$, 0.15 M NaCl, and 0.02% Triton X-100 at pH 8.5 at 4 °C. The protein solution was concentrated to about 6 mg/mL. Glycerol was added to 20%, and enzymes were stored at −80 °C.

The supernatants from the preparations for Lys47Cys/Cys115Ser or Lys213Cys/Cys115Ser double-mutated truncated forms of *E. coli* PBP 5 were individually purified first on an HiTrap SP HP ion exchange column (1.6 × 2.5 cm; Amersham Biosciences Co., Piscataway, NJ), which was equilibrated with 50 mM Mes buffer (pH 5.6). The flow-through fraction was collected at a flow rate of 5 mL/min, and the column was eluted with 250 mL of 50 mM Mes (pH 5.6), 0.5 M NaCl, and 0.02% Triton X-100 of a linear gradient (0 to 0.5 M NaCl). Fractions containing the protein were combined and dialyzed against 50 mM $NaHCO_3$, 0.15 M NaCl, and 0.02% Triton X-100 at pH 7.5. Then, the samples were loaded onto a Sephadex G-50 (Pharmacia Biotech, Piscataway, NJ) size-exclusive column (2.5 × 50 cm), which was pre-equilibrated with 50 mM $NaHCO_3$, 0.15 M NaCl, and 0.02% Triton X-100 at pH 7.5. The protein was eluted with 100 mL of the same buffer at a flow rate of 1.6 mL/min. Fractions containing the desired protein were combined and dialyzed against 25 mM $NaHCO_3$, 0.15 M NaCl, and 0.02% Triton X-100 at pH 8.5. All steps were performed at 4 °C. The protein fractions collected were subsequently concentrated in a Stirred Ultrafiltration Cells (Amicon, Danvers, MA). The concentration of the protein was determined spectrophotometrically using the BCA Protein Detection Kit (Pierce). SDS−PAGE showed that the purity of all of the desired proteins was more than 95%. Glycerol was added to 20%, and the enzymes were stored at −80 °C.

Chemical Modification of the Cys47Ser/Cys115Ser or Cys213Ser/Cys115Ser Mutant Protein. A modified version of the method of Golemi et al. (*7*) was used for the chemical modification. A total of 8 mg of the double-mutant tPBP 5 was denatured in 8 M urea, 200 mM AMPSO, and 15 mM EDTA at pH 8.5, in a final volume of 10 mL. The exposure of cysteine to solution was assessed by its titration (30 μL aliquot of the denaturation mixture) with DTNB, per the method of Ellman (*9*, *10*). The mixture was kept at 25 °C with gentle mixing under an atmosphere of argon for 30 min. Upon full denaturation, the protein was incubated with a freshly prepared solution of 2-bromoethylamine in the denaturing buffer that provided a final concentration of 50 mM. The mixture was then gently mixed for about 20 h at 25 °C, at which point the cysteine was fully modified (assessed by DTNB titration). The enzyme was diluted in 100 mM sodium phosphate, 100 mM ammonium sulfate, and 0.001% Triton X-100 at pH 8.5 (refolding buffer; total volume of 500 mL) and was gently mixed for 90 min at 4 °C. Removal of urea and ammonium sulfate was accomplished by extensive dialysis against 25 mM $NaHCO_3$, 0.15 M NaCl, and 0.02% Triton X-100 at pH 9.0 in three steps (60, 30, and 0 mM ammonium sulfate). The protein was concentrated to about 2.5 mg/mL.

Isoelectric Focusing. Ampholine PAGplate (pH 3.5−9.5) was purchased from GE Healthcare (Piscataway, NJ). The gel was run using Multiphor II Electrophoresis System (Amersham Pharmacia Biotech, Picataway, NJ) according to its protocol.

DD-Carboxypeptidase Assays. The carboxypeptidase activity was monitored by a modified fluorescence-based assay method described previously (*11*). The standard assay mixture (40 μL) consisted of buffer (pH 4.5−12; see below), 150 mM NaCl, 0.5 mg/mL BSA, carboxypeptidase substrate diacetyl-L-Lys-D-Ala-D-Ala, and 0.3−2.5 μM PBP 5. Buffers for the pH range of 4.5 to 12 were 150 mM sodium citrate (pH 4.5−6.0), sodium phosphate (pH 6.5−9.0), and Caps (pH 9.0−12). Assays were monitored for 30 min at 25 °C. The reaction was stopped by the addition of the detection reagent (360 μL) containing 0.55 mg/mL ampicillin (0.5 mg/mL in 400 μL of final assay volume), 10 μL of QuantaBlu substrate solution, 1.0 units of HRP, 2.78 μg/mL FAD (2.5 μg/mL in 400 μL final assay volume), and 0.06 units of DAO in 0.1 M Tris at pH 8.5. Fluorescence was detected after a 60-min development with the excitation wavelength of 325 nm and emission of 410 nm. Fluorescence was determined by a Cary Eclipse Fluorescence Spectrophotometer (Mulgrave Victoria, Australia). Fluorescence was converted to quantity of D-Ala in the mixture according to a standard curve for D-Ala. Control experiments with PBP 5 in the absence of substrate and with substrate in the absence of PBP 5 were included for all experiments. Protein concentrations were determined by BCA assays (Pierce) according to the manufacturer's procedure.

The kinetic parameters were fitted to the Michaelis−Menten enzyme kinetics equation by nonlinear regression using GraFit 4.0 (Erithacus Software, Staines, U.K.).

$$v = \frac{V_{max}[S]}{K_m + [S]} \quad (1)$$

The following equation for the double ionization model was used to fit the data:

$$k_{obs} = \frac{k_{lim1} \times 10^{(pK_1 - pH)} + k_{lim2}}{1 + 10^{(pK_1 - pH)} + 10^{(pH - pK_2)}} \quad (2)$$

The pH dependence of k_{cat} and k_{cat}/K_m were fitted to the double ionization bell model using GraFit 4 (Erithacus Software Ltd.).

Computational Analyses. The wild-type PBP 5 (PDB code, 1NZO) X-ray structure was used for these studies. The general procedures for calculating pK_a values for amino acids were reported previously (*7*). The three-step procedure involved the preparation of an explicitly solvated enzyme complex, molecular dynamics equilibration of the complex, and configuration of a thermodynamic cycle and evaluation

of the free-energy variations by the thermodynamics integration method (*12*).

The enzyme structure was prepared using SYBYL 7.0 (Tripos Inc.), and the protonation of residues was carried out using the xleap program in AMBER (*13*). The enzyme was then fully solvated along with the 190 water molecules from the X-ray structure by generating a rectangular box containing about 66,820 and 66,142 atoms, respectively, for Lys47 and Lys47···H_2O systems. The TIP3P model (*14*) was used for water, and the particle mesh Ewald (PME) method was applied to account for the long-range electrostatic interactions (*15*). Atomic charges of the residues in the enzyme−water complex were assigned with AMBER parm99 parameters, and the charges for the hydroxyl anion were determined using an HF/6-31G(d) optimization calculation and a two-stage electrostatic potential fitting procedure (*16*).

The equilibration was started by minimizing the energy of the water molecules, while restraining, with harmonic potentials, 5428 and 5430 atoms of the Lys47 and Lys47···H_2O systems, respectively. A molecular dynamics simulation was then carried out at 300 K, which includes five 20 ps runs and two 200 ps runs. The thermodynamic integration method implemented in the AMBER package was used to calculate the free-energy variation for the protonation of Lys47 (abbreviated AH^+) (*17*). This protonation reaction constitutes one half of a thermodynamic cycle. The other half of the cycle was supplemented with the protonation of Lys306 (BH^+), a surface lysine residue with expected unperturbed pK_a. In the complete thermodynamic cycle, pK_a(AH^+) is calculated by

$$\mathrm{p}K_a(\mathrm{AH}^+) = 0.729\Delta G + \mathrm{p}K_a(\mathrm{BH}^+) \quad (3)$$

where $\Delta G = \Delta\Delta G_{aq}(\mathrm{A} - \mathrm{AH}^+) - \Delta\Delta G_{aq}(\mathrm{B} - \mathrm{BH}^+)$ (in kcal·mol^{-1}). The constant 0.729 is the value of 1/(2.303*RT*) with gas constant $R = 1.984 \times 10^{-3}$ kcal·K^{-1}·mol^{-1}, temperature $T = 300$ K, and p$K_a(\mathrm{BH}^+) = 10.8$ for the unperturbed surface lysine in the aqueous milieu.

The thermodynamic free-energy integration method was applied to evaluate $\Delta\Delta G_{aq}(\mathrm{X} - \mathrm{XH}^+)$ with $X = \mathrm{A}$ or B, which is the free-energy difference between the unprotonated state X and protonated state XH^+,

$$\Delta\Delta G_{aq}(\mathrm{X} - \mathrm{XH}^+) = \Delta\Delta G_{aq}(\mathrm{X}) - \Delta\Delta G(\mathrm{XH}^+) \quad (4)$$

With the thermodynamic integration method, the difference is accurately evaluated with a 12-point Gaussian quadrature

$$\Delta\Delta G(\mathrm{X}(\lambda = 0) - \mathrm{XH}^+(\lambda = 1)) = \int_0^1 \left\langle \frac{\partial V(\lambda)}{\partial \lambda} \right\rangle_\lambda d\lambda = \sum_{i=1}^{12} w_i \left\langle \frac{\partial V(\lambda)}{\partial \lambda} \right\rangle_{\lambda_i} \quad (5)$$

where w_i and λ_i are known (*13*), and $\partial V/\partial\lambda$ is determined with the free energy perturbation theory (explained below). Sampling over the 12 Gaussian points was completed with a 50 ps molecular dynamics simulation, one 10 ps dynamic sampling, and two 20 ps dynamic averaging. A 20-point Gaussian quadrature (*18*) resulted in similar values.

RESULTS AND DISCUSSION

Lysine 47 of PBP 5 finds counterparts in all other serine-dependent PBPs and β-lactamases. The side chain of this residue is in hydrogen-bonding contact with that of Ser44, the catalytically important serine (Figure 2). The pK_a of the corresponding lysine in the TEM-1 β-lactamase of *E. coli* has been evaluated at 8.0−8.5 (*7*), and its role in promotion of serine for acylation by the substrate is now documented using high-level molecular orbital calculations (*19*).

The use of γ-thialysine variants of enzymes allows construction of proteins that are virtually native in character, except that the presence of the γ-sulfide group perturbs the pK_a of the amine in the residue (*7*, *20*−*25*). The pK_a of the side chain amine of the amino acid *N*-acetyl-γ-thialysine is lowered to 9.4−9.5, an attenuation of approximately one p*K* unit compared to that of lysine (*7*, *26*, *27*). If the lysine that is being substituted by γ-thialysine were to be critical in the catalytic events that are being evaluated, its influence will be detected in the discrete catalytic steps that would be perturbed. For this purpose, γ-thialysine is introduced at a specific position in a given protein by a combination of site-directed mutagenesis (lysine converted to cysteine) and the requisite modification of the reactive side chain thiol of the cysteine by bromoethylamine to generate γ-thialysine.

As shown in Figure 2, the active site of PBP 5 of *E. coli* has two lysine residues, Lys47 and Lys213. We set out to elucidate the roles of these two lysines in catalysis by PBP 5 by the preparation of the γ-thialysine mutants at the respective positions. A number of considerations went into the experimental design. First, we realized that these lysines are buried residues with no direct solvent contact. For example, once the Lys47Cys mutant variant is correctly folded, the cysteine thiol would not be accessible to bromoethylamine, the reagent that modifies it to generate the γ-thialysine residues. Hence, we would be in need of denaturing the protein, chemically modifying it, and then refolding it for the study. Refolding of single-domain proteins is significantly less complicated than that of multidomain proteins. As such, we opted to clone only the catalytic domain of PBP 5, which closely resembles class A β-lactamases and dispensed with the domain of the unknown function and the membrane anchor (Figure 2) (*28*). This soluble version of PBP 5 lacking the extra domains is referred to as the truncated wild-type PBP 5 (or twtPBP 5) hereon. This truncated enzyme contains a single cysteine, Cys115, which had to be replaced before the generation of the cysteine mutant variant at position 47. We prepared the Cys115Ser mutant variant of the catalytic domain. We state parenthetically that we expressed and purified this mutant variant and showed by kinetic experiments that it was identical in its catalytic activity to twtPBP 5. This result agreed well with a previous study (*29*), showing that this residue is not essential for the enzyme function. We have retained this mutation in the other proteins that we have studied, and we refer to this variant as the truncated PBP 5 (or tPBP 5). Subsequently, we prepared the Lys47Cys and Lys213Cys mutant variants of tPBP 5. Both proteins were devoid of activity (1.5% and 1.7% of the tPBP 5 activity, respectively), underscoring the importance of each of these two residues in enzyme function. The findings from site-directed mutagenesis at Lys47 by others are consistent with our observation (*30*, *31*). Furthermore, on denaturation of the protein in 8 M urea, we were able to titrate 1.0 equiv of thiol (the cysteine side chain) per protein molecule by the use of DTNB.

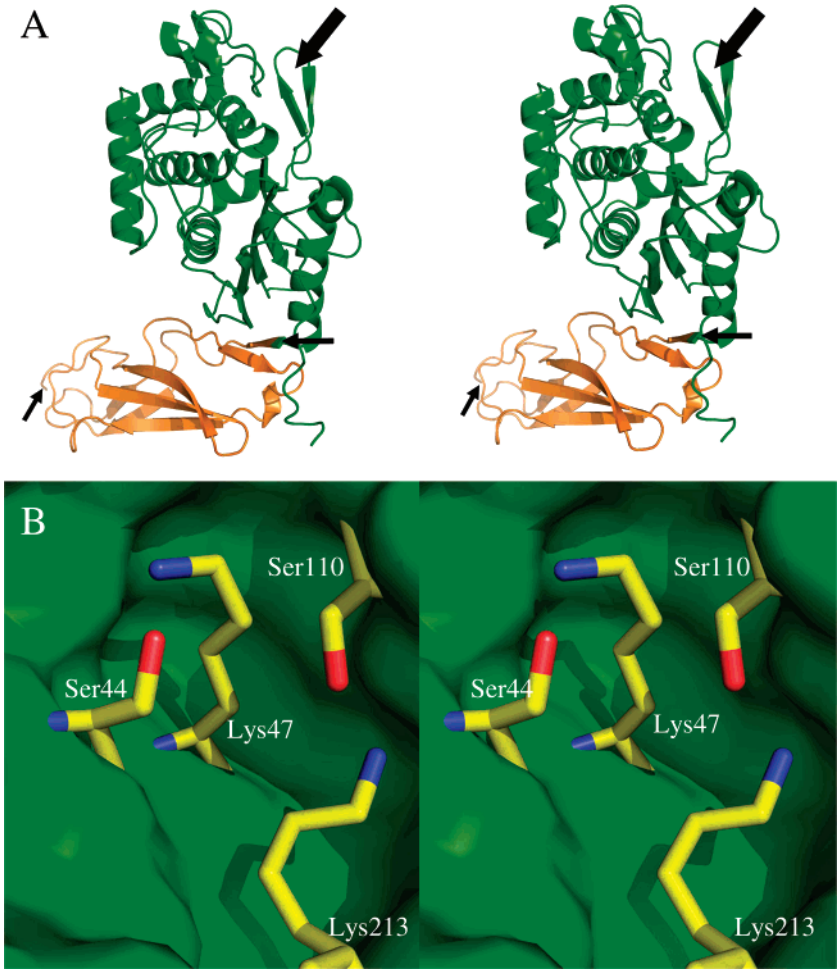

FIGURE 2: Structure of penicillin-binding protein 5 of *E. coli* and its active site. (A) Stereoview of a ribbon representation of the three-dimensional structure of penicillin-binding protein 5 (PBP 5) from X-ray crystallography (PDB code: 1ZNO). The truncated domain that was used in this study is shown in green (the arrow at four o'clock points to the truncation site), and the rest of the protein is shown in orange. The arrow at seven o'clock points to the C-terminus domain of the protein, which is anchored to the inner membrane. (B) Stereoview of the active site of PBP 5 showing the conserved residues of the Ser-Lys dyad (Ser44 and Lys47) as well as other highly conserved residues. The residues are shown in capped-sticks representation with atoms colored according to atom types. (C, N, and O are shown in yellow, blue, and red, respectively). A Connolly surface is constructed around the active site to facilitate viewing.

We denatured twtPBP 5 and refolded it according to the procedure of Golemi et al. (*7*). We were able to document that we recovered full activity during this process. This gave us confidence that after chemical modification of the denatured Lys47Cys and Lys213Cys mutant variants of tPBP 5, the likelihood of success in reconstituting the γ-thialysine mutant variant was high. Accordingly, the reaction of Lys47Cys and Lys213Cys mutant variants of tPBP 5 with bromoethylamine in the AMPSO buffer under an atmosphere of argon proceeded to quantitative completion, according to titration of the cysteine thiol at 25 °C by DTNB. We used isoelectric focusing gel electrophoresis to look at the extent of protein modification under these conditions. Isoelectric focusing showed that the modified double mutants were each single species; hence, the chemical reaction simply modified the cysteine residue in each case (lack of a thiol and a single species by isoelectric focusing). Therefore, the chemical modification step was indeed selective for reaction at the cysteine thiol. The resultant modified proteins were individually refolded to result in the fully constituted Lys47γ-thialysine and Lys213γ-thialysine variants of PBP 5 (referred to as γtPBP 5 hereafter). The Lys47γ-thialysine and Lys213γ-thialysine mutant variants of tPBP 5 exhibited approximately 40% and 10%, respectively, of the activity of twtPBP 5 at optimal pH. The Lys73γ-thialysine variant of the TEM-1 β-lactamase exhibited approximately 50% of the wild-type activity (*7*). The overall attenuation of activity for the γ-thialysine mutant variants can be attributed to the perturbation of the catalytic process by the γ-thialysine residue, as will be described.

With the Lys47γ-thialysine and Lys213γ-thialysine mutant variants in hand, we set out to evaluate them in kinetic experiments. A difficulty in the assay of this enzyme is the fact that the peptidoglycan substrate for the enzyme is actually a polymer. Unfortunately, this presents a logistical problem in that the polymeric substrate is not available in a pure state for quantitative analyses with the enzyme. Furthermore, the synthetic samples of fragments of the peptidoglycan are not easily obtained, hence the quantities needed for kinetic determination are not available. As a compromise, we and others (*11*, *30*) have used diacetyl-L-Lys-D-Ala-D-Ala. Whereas diacetyl-L-Lys-D-Ala-D-Ala does serve as a substrate, it is a relatively poor substrate for PBP 5.

The profiles of k_{cat}/K_m and k_{cat} for the hydrolysis of diacetyl-L-Lys-D-Ala-D-Ala were characterized from pH 4.5

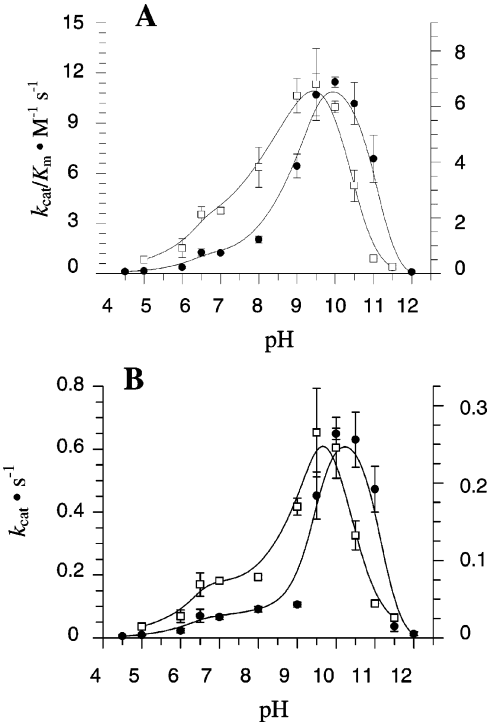

FIGURE 3: pH profiles of k_{cat}/K_m (A) and k_{cat} (B) of the wild type (tPBP 5; ●; left *y*-axis) and of Lys47γ-thialysine (□; right *y*-axis) PBP 5. The error bars in the plots represent the standard errors for each data point. All data points are the average of three determinations, and the point-spreads are indicated by error bars in each case.

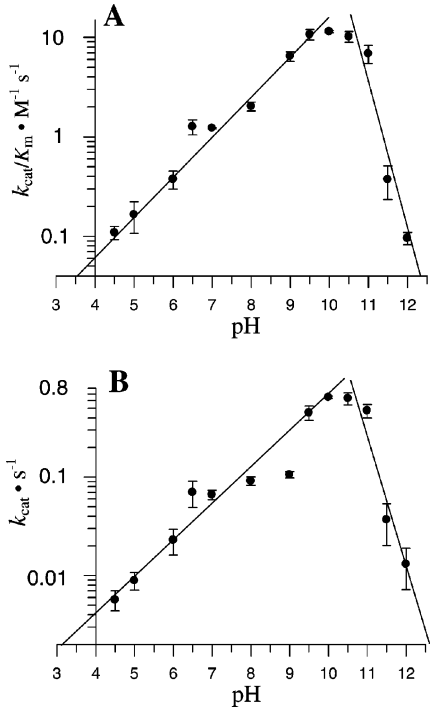

FIGURE 4: Plots of log(k_{cat}/K_m) (A) and log(k_{cat}) (B) vs pH of the wild type (tPBP 5). The titration at 6.1 appears as a bump on an otherwise linear set of data points. The error bars in the plots represent the standard errors for each data point. All data points are the average of three determinations, and the point-spreads are indicated by error bars in each case.

to 12. This pH range allowed both acidic and basic limbs of the pH profile to be observed. The tPBP 5 shows optimal catalysis at approximately pH 9.5−10.5 (Figure 3A and B). Controls with substrate in the absence of tPBP 5 or with tPBP 5 in the absence of substrate had no measurable activity.

The pH dependence of k_{cat}/K_m of the tPBP 5, an indicator of the state of the free enzyme or the substrate, revealed three titratable residues with pK_a values of 6.1 ± 0.4, 9.1 ± 0.1, and 10.8 ± 0.1. The pH dependence of k_{cat}, an indicator of the complex of enzyme and the substrate, for tPBP 5 revealed three titrations as well, with pK_a values of 6.1 ± 0.3, 9.8 ± 0.2, and 10.7 ± 0.2. The three titrating residues are clearly the same in both the free enzyme and in the complex with the substrate. Because the low-pH titration is not seen in studies of the full-length protein (*30*), the observation suggests that it is due to a residue at the interface of the two domains (observed in our truncated protein). Furthermore, its contribution to the activity profile is very small; hence, this titration will not be discussed hereafter. We hasten to add that tPBP 5 also experiences a somewhat reduced k_{cat} value compared to that of the full-length enzyme (*30*). Therefore, domain 2, whose function is not known, would appear to enhance the DD-carboxypeptidase activity somewhat. The other two titratable residues are both in the alkaline range and are likely to be due to the two lysines within the active site. *The important conclusion from these experiments is that assuming that these titrations are due to the lysine residues at optimal catalysis, one lysine is in its free-base form (titrating from pH 8−10), and the other is in its protonated form (titrating from pH 10−12).*

The plots of log(k_{cat}) or log(k_{cat}/K_m) versus pH reveal how many residues contribute to the titration events in the enzyme−substrate complex or in the free enzyme, respectively (*32*). The values of the slopes at the two titrating limbs indicate the number of residues that contribute to each. These data are given in Figure 4, indicating that with a slope of close to 1 for the lower-pH limb for both plots, that limb is due to the titration of a single residue. The higher-pH limb is being contributed to potentially by as many as three residues, as will be discussed more fully below. Its slope is three times that of the other.

For the γ-thialysine47 variant, we see the same three titratable residues (Figure 3). However, as an unexpected observation, the perturbed pK_a of residue 47 in this mutant variant is manifesting its effect at both limbs of the bell-shaped profile. The γ-thialysine47 variant gave pK_a values of 8.1 ± 0.3 and 10.1 ± 0.2 for the k_{cat}/K_m profile and values of 9.2 ± 0.4 and 10.2 ± 0.3 for the k_{cat} profile for the bell-shaped part of the plots. This indicates a change in the pK_a of approximately 0.6−1.0 for the lower-pH limb and one of 0.5−0.7 for the higher-pH limb. The effect of the pK_a perturbation is close to the maximum to be expected for the lower-pH limb and somewhat less for the higher-pH limb.

As indicated above, the lower-pH limb of the bell-shaped plot is due to a single residue titrating, and it would appear from the experiment of Figure 3 that the residue is Lys47. Hence, Lys47 in its *free base* form contributes optimally to catalysis. Because the side chain amine of Lys47 is in contact with the hydroxyl group of Ser44 in the X-ray structure, it is the free-base Lys47 that promotes Ser44 for acylation by the substrate. We propose that Lys47 is also a contributor to the higher-pH limb of catalysis by promoting a water molecule for the deacylation step (discussed in greater detail later). Hence, the smaller perturbation for catalysis at this stage is due to the complex of the free-base amine of Lys47 with a water molecule. The water molecule will be promoted

to give deacylation of the acyl-enzyme species. Hence, PBP 5 enjoys symmetry in catalysis, and Lys47 activates the Ser44 hydroxyl for the formation of the acyl-enzyme species. It also promotes a water molecule in the second step to give the hydrolytic deacylation of the acyl-enzyme species.

The data in Figure 5 argue that Lys213 contributes to the higher-pH limb of catalysis in the bell-shaped region. The pK_a perturbation of γ-thialysine213 (as much as 0.8 pH units) is seen only for the k_{cat}/K_m profile (free enzyme) and not for the k_{cat} profile (the enzyme−substrate complex). This means that the perturbation of the pK_a is compensated in the enzyme−substrate complex to diminish its contribution to the overall catalysis. Hence, Lys213 is protonated for optimal catalysis because enzyme activity is lost during titration of this residue in the direction of higher pH. The measured pK_a for Lys213 indicates that this residue is largely a typical lysine in contrast to the case of Lys47 whose pK_a has been attenuated. The protonated Lys213 and the Lys47···H_2O complex both contribute to the higher-pH limb of catalysis. The slope of the higher-pH limb of the plots in Figure 4 argues that there might yet be another residue besides Lys213 and the Lys47···H_2O complex contributing to the higher-pH limb. However, this must be a residue outside the active site, perhaps contributing to enzyme stability in its protonated form.

The availability of high-resolution (1.6−2.5 Å) structures for PBP 5 presented the opportunity to evaluate the pK_a values for Lys47 and for the Lys47···H_2O complex by computation. This has been done by the state-of-the-art computational treatment using the molecular dynamics-based thermodynamic integration method. This method has been shown to reproduce the experimental value for the free-energy change within 1 kcal/mol (*33*).

Several factors in this method are instrumental in resulting in highly accurate determinations for pK_a of ionizable groups. These include accounting for protein flexibility, explicit treatment of water and counter ions, and the use of the AMBER force field for electrostatics and van der Waals interactions surrounding the ionizable residues. The solvated structure for PBP 5 was treated with PME for the treatment of long-range electrostatics to preserve the environment of Lys47.

The value of pK_a is related to the free-energy difference between the protonated and the unprotonated states. The thermodynamics cycle shown below was used for these calculations. The deprotonation reaction constitutes the full thermodynamic cycle for free-energy variations in aqueous condition, which forms the basis for eqs 3−5 used to calculate the pK_a of Lys47 (*34*): where AH^+ corresponds to

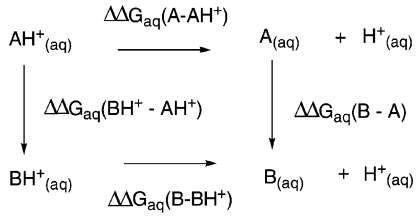

the protonated Lys47, and BH^+ is the protonated Lys306. The pK_a value of Lys306 is expected to be that of a typical lysine (because it is a surface residue), and eqs 3−5 can be used to calculate the pK_a of Lys47, given that $\Delta\Delta G_{aq}$(B − BH^+) and $\Delta\Delta G_{aq}$(A − AH^+) are known. These free-energy terms were computed using the thermodynamic integration method. In general, the difference of free energy between two states (in this case, protonated and unprotonated) can be determined, if a statistical ensemble of structures is available for both states. However, the energy difference between states can numerically be large and might lead to inaccuracies in the free-energy calculation. One solution to this problem (*12*) was the introduction of a series of non-physical intermediate states joining the two physical states. These intermediate states are defined by introducing a coupling parameter $0 < \lambda < 1$ with $\lambda = 0$ for the protonated state (P) and $\lambda = 1$ for the unprotonated state (U), for which the potential energy (*13*) is defined by eq 6.

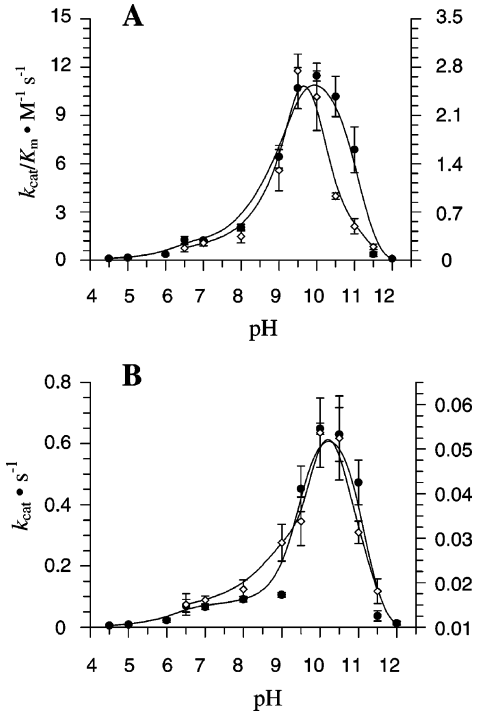

FIGURE 5: pH profiles of k_{cat}/K_m (A) and k_{cat} (B) of the wild type (tPBP 5; ●; left *y*-axis) and of Lys213γ-thialysine (open rhombus; right *y*-axis) PBP 5. The error bars in the plots represent the standard errors for each data point. All data points are the average of three determinations, and the point-spreads are indicated by error bars in each case.

$$V(\lambda) = (1 - \lambda)V_P + \lambda V_U \qquad (6)$$

Generally, $V(\lambda)$ is continuous, and its derivative is assumed to exist for all λ values in the framework of free-energy perturbation theory (*13*). Calculation of the free-energy difference between the protonated and unprotonated states of Lys47 and of Lys306 (an internal reference) using the thermodynamic integration methods thus consists of collecting an ensemble of structures using molecular dynamics simulations at λ_i ($i = 1$ to 12) and using a 12 point Gaussian quadrature to determine the integral in eq 5.

The difference between $\Delta\Delta G_{aq}$(B − BH^+) and $\Delta\Delta G_{aq}$(A − AH^+) for the proton transfer between Lys47 and Lys306 was found to be −2.89 kcal/mol. Using eqs 3−5, along with the known pK_a of 10.8 for a typical lysine such as Lys306, the computed pK_a of Lys47 was found to be 9.1 ± 0.2 (determined in triplicate). The method is known to give standard deviations in the range of ±(0.05−0.20) pK units

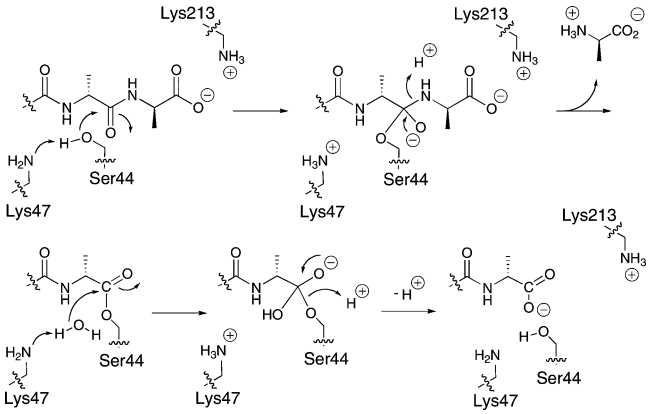

FIGURE 6: Involvement of Lys47 and Lys213 in the catalytic events of PBP 5. Lysine 213 anchors the substrate by the electrostatic draw of the terminal carboxylate of the substrate to the protonated side chain of the residue. As Lys47 activates Ser44, it shuttles the proton to the nitrogen of the departing terminal D-Ala, whereby it reverts back to the free-base state. The free-base Lys47 now promotes a water molecule for the deacylation step; hence, PBP 5 enjoys symmetry in catalysis. The proton from the water molecule is shuttled to the departing serine Oγ, returning Lys47 to its ground-state free-base form. Each step goes through a tetrahedral species, which is ensconced in the so-called oxyanion hole created by the backbone nitrogens of Ser44 and His217.

(*35*). The calculated pK_a value is in excellent agreement with the experimentally determined pK_a of 9.1 ± 0.1 for the free enzyme.

We have invoked a symmetric catalytic scheme for PBP 5. In the second step of catalysis, Lys47 promotes a water molecule for deacylation of the acyl-enzyme species. In light of the observed contribution of Lys47 to both limbs of the bell-shaped portion of the catalytic profile (Figure 3), we wondered whether the lysine complex to a water molecule would collectively have a pK_a that would contribute to the profile. To answer this question, we resorted to the use of molecular dynamics simulation and the free-energy integration method. In terms of the previous notation, AH^+ is for protonated Lys47-HO^- and BH^+ for protonated Lys306-HO^-. To simulate the reaction, [protonated Lys47-HO^-]$_{aq}$ → [free-base Lys47-HO^-]$_{aq}$ + H^+_{aq}, a multistage averaging molecular dynamics scheme was applied after the enzyme and water complex were warmed to 300 K. The analysis led to the computed value of the pK_a of the lysine/water complex at 10.7 ± 0.3, in excellent agreement with the experimental pK_a value of 10.8 ± 0.1.

The mechanistic findings in this article are summarized in Figure 6. Both Lys47 and Lys213 contribute to catalysis. Lysine 47 is intimately involved in the proton-transfer events of the promotion of Ser44 for the acylation event and activation of the hydrolytic water molecule in the second step of the catalytic process. For these roles, it has to exist in a free-base form, and our experimental and computational results unequivocally indicate that at optimal pH for catalysis, Lys47 does exist in the free-base form.

As a sidebar, the information on Lys47 of PBP 5 can be put in perspective with the findings of the related TEM-1 β-lactamase (both from *E. coli*). Lysine 73 of the TEM-1 β-lactamase corresponds to Lys47 of PBP 5, yet three ultrahigh-resolution X-ray structures for class A β-lactamases reveal Lys73 as protonated (*36*−*38*). We showed by the generation of γ-thialysine, by NMR experiments and by computations, that the pK_a for Lys73 of TEM-1 β-lactamase was 8.0−8.5, which also indicated that at the optimal pH for its catalysis this residue is protonated (*7*). In the evolution of the deacylation mechanism in class A β-lactamases, including the TEM-1 β-lactamase, Glu166 was incorporated onto an Ω-loop that exists at the active site. Glu166 promotes a water molecule to give deacylation in the second step of catalysis. This close spatial proximity of Glu166 to Lys73 brings the Lys73 side chain to a protonated form for electrostatic reasons (*19*). We have disclosed on the basis of ab initio QM/MM calculations that in the course of catalysis the ion pair of Lys73-Glu166 would transiently revert to a free-base Lys73 and a protonated Glu166 (*19*). The mechanistic role for the free-base Lys73 from this point on into the process of active-site acylation by the substrate for the TEM-1 β-lactamase is the same as that proposed in this article for PBP 5. As such, the broader mechanistic details between the TEM-1 β-lactamase and PBP 5 for the acylation event are unchanged. This and other mechanistic issues regarding class A β-lactamases have been discussed at length in two recent publications (*7*, *19*; and the citations given therein).

According to our findings, Lys213 exists in its protonated form during optimal catalysis. An earlier crystallographic study had argued that Lys213 in its free-base state (through a chain of three water molecules) could promote the hydrolytic deacylation of the acyl-enzyme species (*28*). This assertion is inconsistent with the findings reported herein. Whereas the pK_a value for Lys234 of the TEM-1 β-lactamase, counterpart to Lys213 of PBP 5, has not been evaluated by this method (*7*), it is likely that this residue is also protonated (*39*, *40*). Hence, we argue that both Lys213 of PBP 5 and Lys234 of the TEM-1 β-lactamase serve the same role in hydrolysis of their respective substrates, namely, substrate anchoring. Both the carboxylate in the β-lactam antibiotics and the terminal D-Ala carboxylate in the peptidoglycan are drawn electrostatically to the protonated lysines in the two enzymes. This anchoring function is critical for the predisposition of the substrate within the active site for the catalytic events to ensue.

This article documents that mere mutagenesis and analysis by kinetics does not necessarily reveal the nature of the catalytic events. We take it for granted that the change in a residue critical for the events within the active site of an enzyme should abrogate activity, and that is the expected outcome for mutagenesis at the critically important Lys47 and Lys213 of PBP 5. However, perturbation of pK_a, as perfomed in the present study by conversion of the individual lysine residues to γ-thialysine, clearly allows for the dissection of the discrete events.

The role of the lysine in the sequence motif Ser-X-X-Lys has now been evaluated by generation of γ-thialysine for PBP 5 and previously for the TEM-1 β-lactamase (*7*; and citations given therein): one an enzyme that turns over the peptidoglycan and the other β-lactam antibiotics, respectively. It is highly likely that the role of the conduit for proton in the course of catalysis by this conserved residue is the same in other related enzymes.

REFERENCES

1. Massova, I., and Mobashery, S. (1998) Kinship and diversification of bacterial penicillin-binding proteins and beta-lactamases, *Antimicrob. Agents Chemother. 42*, 1−17.
2. Kotra, L. P., Samama, J. P., and Mobashery, S. (2002) *Bacterial Resistance to Antimicrobials, Mechanisms, Genetics, Medical Practice and Public Health* (Lewis, A., Salyers, A., Haber, H., and Wax, R. G., Eds.) pp 123−159, Marcel Dekker Inc., New York.
3. Knox, J. R., Moews, P. C., and Frere, J. M. (1996) Molecular evolution of bacterial beta-lactam resistance, *Chem. Biol. 3*, 937−947.
4. Fisher, J. F., Meroueh, S. O., and Mobashery, S. (2005) Bacterial resistance to beta-lactam antibiotics: compelling opportunism, compelling opportunity, *Chem. Rev. 105*, 395−424.
5. Meroueh, S. O., Bencze, K. Z., Hesek, D., Lee, M., Fisher, J. F., Stemmler, T. L., and Mobashery, S. (2006) Three-dimensional structure of the bacterial cell wall peptidoglycan, *Proc. Natl. Acad. Sci. U.S.A. 103*, 4404−4409.
6. Nelson, D. E., and Young, K. D. (2001) Contributions of PBP 5 and DD-carboxypeptidase penicillin binding proteins to maintenance of cell shape in Escherichia coli, *J. Bacteriol. 183*, 3055−3064.
7. Golemi-Kotra, D., Meroueh, S. O., Kim, C., Vakulenko, S. B., Bulychev, A., Stemmler, A. J., Stemmler, T. L., and Mobashery, S. (2004) The importance of a critical protonation state and the fate of the catalytic steps in class A beta-lactamases and penicillin-binding proteins, *J. Biol. Chem. 279*, 34665−34673.
8. Lee, M., Hesek, D., Suvorov, M., Lee, W., Vakulenko, S., and Mobashery, S. (2003) A mechanism-based inhibitor targeting the DD-transpeptidase activity of bacterial penicillin-binding proteins, *J. Am. Chem. Soc. 125*, 16322−16326.
9. Eyer, P., Worek, F., Kiderlen, D., Sinko, G., Stuglin, A., Simeon-Rudolf, V., and Reiner, E. (2003) Molar absorption coefficients for the reduced Ellman reagent: reassessment, *Anal. Biochem. 312*, 224−227.
10. Wright, S. K., and Viola, R. E. (1998) Evaluation of methods for the quantitation of cysteines in proteins, *Anal. Biochem. 265*, 8−14.
11. Gutheil, W. G., Stefanova, M. E., and Nicholas, R. A. (2000) Fluorescent coupled enzyme assays for D-alanine: application to penicillin-binding protein and vancomycin activity assays, *Anal. Biochem. 287*, 196−202.
12. Hummer, G., and Szabo, A. (1996) Calculation of free-energy differences from computer simulations of initial and final states, *J. Chem. Phys. 105*, 2004−2010.
13. Case, D. A., Darden, T. A., Cheatham,, T. E., III, Simmerling, C. L., Wang, J., Duke, R. E., Luo, R., Merz, K. M., Wang, B., Pearlman, D. A., Crowley, M., Brozell, S., Tsui, V., Gohlke, H., and Mongan, J., Hornak, V., Cui, G., Beroza, P., Schafmeister, C., Caldwell, J. W., Ross, W. S., and Kollman, P. A. (2002) *AMBER 8 Users' Manual*, University of California, San Francisco, CA.
14. Jorgensen, W. L., Chandrasekhar, J., Madura, J. D., Impey, R. W., and Klein, M. L. (1983) Comparison of simple potential functions for simulating liquid water, *J. Chem. Phys. 79*, 926−935.
15. Darden, T., York, D., and Pedersen, L. (1993) Particle mesh Ewald: an N.log(N) method for Ewald sums in large systems, *J. Chem. Phys. 98*, 10089−10092.
16. Bayly, C. I., Cieplak, P., Cornell, W. D., and Kollman, P. A. (1993) A well-behaved electrostatic potential based method using charge restraints for deriving atomic charges: the resp model, *J. Phys. Chem. 97*, 10269−10280.
17. Maveyraud, L., Golemi-Kotra, D., Ishiwata, A., Meroueh, O., Mobashery, S., and Samama, J. P. (2002) High-resolution X-ray structure of an acyl-enzyme species for the class D OXA-10 beta-lactamase, *J. Am. Chem. Soc. 124*, 2461−2465.
18. Morse, P. M., Eedelyi, A., Gray, M. C., Metroplis, N. C., Rosser, J. B., Thacher, H. C., Jr., Todd, J., Tompkins, C. B., and Tukey, J. W. (1965) *Handbook of Mathematical Functions with Formulas, Graphs, and Mathematical Tables* (Abramowita, M., and Stegun, I. A., Eds.) Dover Publications, Inc., New York.
19. Meroueh, S. O., Fisher, J. F., Schlegel, H. B., and Mobashery, S. (2005) Ab initio QM/MM study of class A beta-lactamase acylation: dual participation of Glu166 and Lys73 in a concerted base promotion of Ser70, *J. Am. Chem. Soc. 127*, 15397−15407.
20. Smith, H. B., and Hartman, F. C. (1988) Restoration of activity to catalytically deficient mutants of ribulosebisphosphate carboxylase/oxygenase by aminoethylation, *J. Biol. Chem. 263*, 4921−4925.
21. Planas, A., and Kirsch, J. F. (1991) Reengineering the catalytic lysine of aspartate aminotransferase by chemical elaboration of a genetically introduced cysteine, *Biochemistry 30*, 8268−8276.
22. Messmore, J. M., Fuchs, D. N., and Raines, R. T. (1995) Ribonuclease-a: revealing structure-function-relationships with semisynthesis, *J. Am. Chem. Soc. 117*, 8057−8060.
23. Highbarger, L. A., Gerlt, J. A., and Kenyon, G. L. (1996) Mechanism of the reaction catalyzed by acetoacetate decarboxylase. Importance of lysine 116 in determining the pKa of active-site lysine 115, *Biochemistry 35*, 41−46.
24. Paetzel, M., Strynadka, N. C., Tschantz, W. R., Casareno, R., Bullinger, P. R., and Dalbey, R. E. (1997) Use of site-directed chemical modification to study an essential lysine in *Escherichia coli* leader peptidase, *J. Biol. Chem. 272*, 9994−10003.
25. Toney, M. D., and Kirsch, J. F. (1989) Direct Bronsted analysis of the restoration of activity to a mutant enzyme by exogenous amines, *Science 243*, 1485−1488.
26. Hermann, P., and Lemke, K. (1968) Ionization and stability constants of copper(2) complexes of some amino acids and their sulfur-containing analogs, *Hoppe-Seyler's Z. Physiol. Chem. 349*, 390−394.
27. Li, C., and Gershon, P. D. (2006) pKa of the mRNA cap-specific 2′-O-methyltransferase catalytic lysine by HSQC NMR detection of a two-carbon probe, *Biochemistry 45*, 907−917.
28. Nicholas, R. A., Krings, S., Tomberg, J., Nicola, G., and Davies, C. (2003) Crystal structure of wild-type penicillin-binding protein 5 from *Escherichia coli*: implications for deacylation of the acyl-enzyme complex, *J. Biol. Chem. 278*, 52826−52833.
29. Nicholas, R. A., and Strominger, J. L. (1988) Site-directed mutants of a soluble form of penicillin-binding protein 5 from *Escherichia coli* and their catalytic properties, *J. Biol. Chem. 263*, 2034−2040.
30. Stefanova, M. E., Davies, C., Nicholas, R. A., and Gutheil, W. G. (2002) pH, inhibitor, and substrate specificity studies on *Escherichia coli* penicillin-binding protein 5, *Biochim. Biophys. Acta 1597*, 292−300.
31. van der Linden, M. P., de Haan, L., Dideberg, O., and Keck, W. (1994) Site-directed mutagenesis of proposed active-site residues of penicillin-binding protein 5 from *Escherichia coli*, *Biochem. J. 303*, 357−362.
32. Tipton, K. F., and Dixon, H. B. (1979) Effects of pH on enzymes, *Methods Enzymol. 63*, 183−234.
33. Rao, B. G., Kim, E. E., and Murcko, M. A. (1996) Calculation of solvation and binding free energy differences between VX-478 and its analogs by free energy perturbation and AMSOL methods, *J Comput.-Aided Mol. Des. 10*, 23−30.
34. Merz, K M., Jr. (1991) Determination of pKas of ionizable groups in proteins: the pKa of Glu 7 and 35 in hen eggs white lysozyme and Glu 106 in human carbonic anhydrase II, *J. Am. Chem. Soc. 113*, 3572−3575.
35. Gouda, H., Kuntz, I. D., Case, D. A., and Kollman, P. A. (2003) Free energy calculations for theophylline binding to an RNA aptamer: Comparison of MM-PBSA and thermodynamic integration methods, *Biopolymers 68*, 16−34.
36. Minasov, G., Wang, X., and Shoichet, B. K. (2002) An ultrahigh resolution structure of TEM-1 beta-lactamase suggests a role for Glu166 as the general base in acylation, *J. Am. Chem. Soc. 124*, 5333−5340.
37. Chen, Y., Bonnet, R., and Shoichet, B. K. (2007) The acylation mechanism of CTX-M beta-lactamase at 0.88 a resolution, *J. Am. Chem. Soc. 129*, 5378−5380.
38. Nukaga, M., Mayama, K., Hujer, A. M., Bonomo, R. A., and Knox, J. R. (2003) Ultrahigh resolution structure of a class A beta-lactamase: on the mechanism and specificity of the extended-spectrum SHV-2 enzyme, *J. Mol. Biol. 328*, 289−301.
39. Lenfant, F., Labia, R., and Masson, J. M. (1991) Replacement of lysine 234 affects transition state stabilization in the active site of beta-lactamase TEM1, *J. Biol. Chem. 266*, 17187−17194.
40. Ellerby, L. M., Escobar, W. A., Fink, A. L., Mitchinson, C., and Wells, J. A. (1990) The role of lysine-234 in beta-lactamase catalysis probed by site-directed mutagenesis, *Biochemistry 29*, 5797−5806.

BI700777X